ELSEVIER

21 February 1997

Chemical Physics Letters 266 (1997) 206–216

CHEMICAL PHYSICS LETTERS

The $S_0 \rightarrow S_4$ transition of jet-cooled fluoranthene: vibronic coupling of S_4 with S_3 [1]

Albert A. Ruth, Manfred T. Wick [2]

Max-Planck-Institut für Biophysikalische Chemie, Abteilung Spektroskopie und Photochemische Kinetik, Am Fassberg, D-37077 Göttingen, Germany

Received 8 October 1996; in final form 28 November 1996

Abstract

The $S_1 \rightarrow S_0$ fluorescence excitation spectrum of fluoranthene in a continuous supersonic jet was measured in the region of the $S_0 \rightarrow S_4$ absorption band. The vibrational structure of S_4 was studied up to excess energies of $\approx 1600\ cm^{-1}$ above the $S_{4,0}$ origin at $\approx 35664\ cm^{-1}$. In total 19 vibronic transitions were observed. The origin of the $S_0 \rightarrow S_4$ absorption band consists of at least two transitions, $S_{0,0} \rightarrow S_{4,0'}$ ($\Gamma_{4,0'} \approx 89\ cm^{-1}$) and $S_{0,0} \rightarrow S_{4,0''}$ ($\Gamma_{4,0''} \approx 79\ cm^{-1}$), whose contributions to the 0, 0 band can be described by Lorentzian line profiles. The lower limit of the lifetime of $S_{4,0}$ was estimated to be $\gtrsim 60$ fs. In the overlapping region of the $S_{4,0}$ absorption band and the $\{S_{3,w}\}$ manifold, fluoranthene exhibits an intermediate-level structure; the vibronic coupling $S_4 \Leftrightarrow S_3$ can be classified as a strong intermediate case.

1. Introduction

The photophysical properties of higher excited singlet states S_n ($n > 1$) of large aromatics like fluoranthene are strongly affected by the type of vibronic coupling $S_n \Leftrightarrow S_{n-1}$. The intramolecular coupling mechanism is governed by the interaction of optically *bright* (index b) zeroth-order states $S^0_{n,v}$ (they carry the oscillator strength of the eigenstate of the system) and a dense manifold of optically *dark* (index d) zeroth-order states $\{S^0_{n-1,w}\}$. The zeroth-order Born–Oppenheimer states $S^0_{n,v}$ and $\{S^0_{n-1,w}\}$ are characterized by their energies E_b and E_d, and their widths γ_b and γ_d, respectively. The observed molecular eigenstates $S_{n,v}$ are given by the linear combination of the bright eigenfunction and the eigenfunctions of the dark manifold, whose coefficients depend on the type of interaction that dominates the coupling. The energies of the states $S_{n,v}$ depend on the size of the intramolecular coupling matrix element V and the energy separation of the zeroth-order states $hc\epsilon = |E_b - E_d|$. The coupling strength and the extent of mixing between two different manifolds is described by the parameters $\lambda_{coupl} = (V/\epsilon)^2$ and $\lambda_{mix} = V^2[\epsilon^2 + \frac{1}{4}(\gamma_b - \gamma_d)^2]^{-1}$ [1]. For strongly coupled manifolds ($\lambda_{coupl} > 1$) in molecules with moderate to large energy gaps $\Delta E_{n,n-1} \equiv E(S_{n,0}) - E(S_{n-1,0})$ two types of vibronic coupling can be distinguished, depending on the spectral density ρ_d of vibronic states $\{S^0_{n-1,w}\}$ in the region of the S_n absorption band [1,2].

[1] In memory of Professor Albert Weller († September 27, 1996).

[2] Present address: Institut für physikalische und theoretische Chemie, Humboldt Universität Berlin, Bunsenstr. 1, 10117 Berlin, Germany.

PII S0009-2614(96)01499-6

1.1. The strong intermediate coupling

In the case of an intermediate-level structure with a high density of states ρ_d, the manifold $\{S^0_{n-1,w}\}$ is not quite uniform. It is composed of a finite subset of zeroth-order vibronic states $\{S^0_{n-1,w}\}_{eff}$ (spectral density ρ_{eff}), whose strong direct coupling with bright states $S^0_{n,v}$ of the same symmetry determines the overall coupling scheme between S_n and S_{n-1} [2,3]. The criterion for the intermediate case is that the mean separation of the effectively coupling states, $\epsilon_{eff} = (\rho_{eff})^{-1}$, is of the order of magnitude of the average coupling matrix element V [1,2]:

$$V\rho_{eff} \approx 1. \tag{1}$$

In the strong intermediate case spectra are expected to exhibit a complex structure of overlapping vibronic transitions, whose (oscillator) strength is due to the prevalent coupling mechanism. The widths $\Gamma_{n,v}$ of the observed eigenstates $S_{n,v}$ depend on the widths and extent of mixing of the zeroth-order states involved. [1] Lifetimes derived from $\Gamma_{n,v}$ can at best be lower limits of the real lifetime $\tau_{n,v}$. The true $S_n \rightarrow S_0$ radiative lifetime τ_{Fn} can be evaluated using

$$\tau_{Fn} = m\tau^*_{Fn}, \tag{2}$$

where m is the estimated number of components of the intermediate-level structure that replaces the zeroth-order 0, 0 transition $S_{0,0} \rightarrow S_{n,0}$ [4–6] and τ^*_{Fn} is the lifetime calculated from the $S_0 \rightarrow S_n$ absorption band.

A typical example for the strong intermediate case is the $S_2 \Leftrightarrow S_1$ coupling of naphthalene [7] with $\Delta E_{2,1} \approx 3900\ cm^{-1}$ in a supersonic jet [8].

1.2. The statistical limit

In the case of the statistical limit the states $\{S^0_{n-1,w}\}$ form a virtually smooth continuum in the spectral region of S_n, and the coupling of the subset $\{S^0_{n-1,w}\}_{eff}$ with the rest of the manifold $\{S^0_{n-1,w}\}$ is strong. Nearly all dark states can be regarded as effective states in this case ($\rho_d \approx \rho_{eff}$) and criterion (1) changes to [2]:

$$V\rho_{eff} \gg 1. \tag{3}$$

This condition is always fulfilled for weakly mixing states with large energy gaps $\Delta E_{n,n-1}$. The 0, 0 transition of a symmetry-allowed $S_0 \rightarrow S_n$ absorption band consists of a single line, whose homogeneous lineshape is Lorentzian [5,9]. The vibronic structure of S_n is unambiguously based on the well defined origin $S_{n,0}$; the lineshapes of vibronic transitions are also homogeneous and Lorentzian. Lifetimes can be calculated using the observed linewidths $\Gamma_{n,v}$, provided pure dephasing and other mechanisms of line broadening do not play a role:

$$\tau_{n,v} = \frac{1}{2\pi c \Gamma_{n,v}}. \tag{4}$$

No exception from the statistical limit is known for the coupling of S_1 with S_0 for large polyatomic molecules. Among aromatic hydrocarbons only few compounds, such as azulene [10], phenanthrene [9,11,12] and coronene [13–15] exhibit $S_2 \Leftrightarrow S_1$ vibronic coupling according to the statistical limit. In a recent publication [16] we showed that the $S_0 \rightarrow S_3$ absorption band of 1,2-benzanthracene satisfies the criteria for the statistical limit of vibronic coupling of S_3 with S_2.

The objective of the present work was to study the vibronic structure of S_4 of jet-cooled fluoranthene in conjunction with the vibronic coupling $S_4 \Leftrightarrow S_3$. The ground state S_0 and the excited singlet states S_n of fluoranthene have already been the subject of several publications [17–20]. The ground state absorption spectrum of fluoranthene in perfluoro-n-hexane at room temperature is shown in Fig. 1. Kolc et al. [19] have shown that six excited singlet states contribute to the absorption spectrum up to $\approx 40000\ cm^{-1}$. Regarding the moderately large energy gap $\Delta E_{4,3} \approx 3750\ cm^{-1}$ in 3-methylpentane [19] one would expect a strong intermediate $S_4 \Leftrightarrow S_3$ coupling for fluoranthene, in accordance with the classic example of the $S_2 \Leftrightarrow S_1$ coupling in isolated naphthalene molecules ($\Delta E_{2,1} \approx 3900\ cm^{-1}$). The decay widths $\Gamma_{4,v}$ of fluoranthene in S_4, however,

[1] Strong coupling implies a strong mixing of states only when the damping term $\gamma_b - \gamma_d$ is reasonably small. Efficient damping in a strong-coupling case, however, can lead to a weak-mixing situation, i.e. states cannot mix efficiently owing to their short lifetimes.

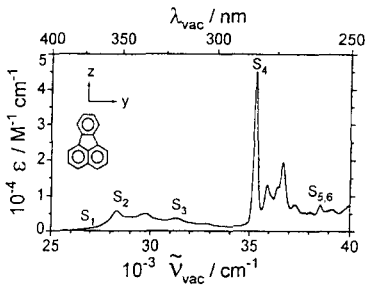

Fig. 1. Absorption spectrum of fluoranthene in perfluoro-n-hexane at 293 K. Approximate locations of the origins of the excited electronic singlet states S_n ($n = 1$–6) are indicated.

are expected to be much broader [16] than for S_2 of naphthalene ($\Gamma_{2,v} \approx 2$ cm^{-1}), which will affect the interstate mixing and thus the prevalent coupling mechanism. Moreover, due to the larger size and lower symmetry of fluoranthene (C_{2v}) as compared to naphthalene (D_{2h}) the density of coupling $S_{3,w}$ states at $S_{4,0}$ is much higher than in the naphthalene case and therefore the coupling is likely to be close to the statistical limit. In this Letter we shall present experimental evidence for the strong intermediate coupling of S_4 with S_3 in isolated fluoranthene, by investigating the $S_0 \rightarrow S_4$ excitation spectrum of the $S_1 \rightarrow S_0$ fluorescence of fluoranthene in a free continuous supersonic jet (compare Fig. 1).

2. Experiment

The jet apparatus employed has been described in detail elsewhere [16,21]. Zone-refined fluoranthene was seeded into a neon stream at a stagnation pressure of ≈ 1000 mbar. The partial pressure of fluoranthene at a temperature of ≈ 368 K was ≈ 0.02 mbar [22]. A circular glass nozzle with a diameter of ≈ 120 μm was used to create the continuous adiabatic expansion. Isolated fluoranthene molecules were excited ≈ 2.8 mm downstream from the nozzle. The fluorescence was collected at right angles relative to the jet and to the excitation laser beam, and was detected with a photomultiplier (EMI 9659 QB). A broadband interference filter with center at $\lambda_{max} \approx 413$ nm (FWHM ≈ 23 nm) was used to suppress the scattered light from the excimer-pumped frequency-doubled pulsed dye laser (Lambda Physik LPX100, FL3002) and to select the $S_1 \rightarrow S_0$ fluorescence at its maximum. The fraction of laser light, reflected at the entrance window of the vacuum chamber, was used to correct for the wavelength dependence and the fluctuations of the photon fluence (the small wavelength dependence of the entrance window's reflection within the excitation range (265–295 nm) was neglected). The reflected light was directed onto a quantum converter (rhodamine B in ethylene glycol [23]), whose fluorescence was measured with a second photomultiplier (Hamamatsu R1464). The signals from both photomultipliers were simultaneously measured with two boxcar integrators (Stanford Research System, SR250) and subsequently divided in order to normalize all spectra to constant photon fluence. Typical sample sizes used were 100 shots per data point.

3. Results and discussion

The excitation spectrum of the $S_1 \rightarrow S_0$ fluorescence of isolated fluoranthene in the range of the $S_0 \rightarrow S_4$ absorption band (34400–37400 cm^{-1}) is shown in Fig. 2. After $S_0 \rightarrow S_4$ excitation and subsequent fast internal conversion $S_{4,v} \rightsquigarrow S_{1,v'}$, the $S_{1,v'} \rightarrow S_{0,v''}$ fluorescence from *highly* vibrationally excited fluoranthene in S_1 (excess energy ≈ hc10400 cm^{-1} above $S_{1,0}$) possesses a sufficient quantum

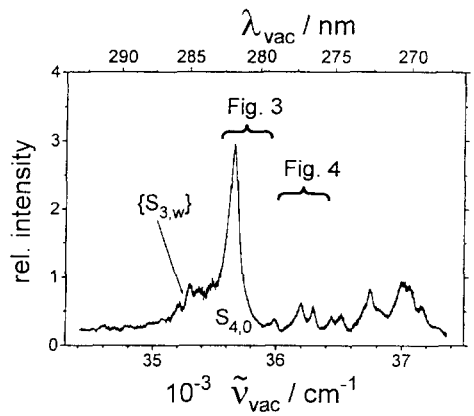

Fig. 2. Excitation spectrum of the $S_{1,v'} \rightarrow S_{0,v''}$ fluorescence of jet-cooled fluoranthene in the spectral region of the $S_0 \rightarrow S_4$ absorption band. Neon was the carrier gas in this adiabatic expansion (also in Figs. 3 and 4). The spectrum is normalized to constant photon fluence.

yield Φ_{S_1} for measuring the excitation spectrum (for fluoranthene in cyclohexane the quantum yield is $\Phi_{S_1} \approx 0.3$ [24]). We assume that the quantum yield of the $S_1 \rightarrow S_0$ fluorescence is approximately independent of the excitation wavenumber in the spectral range of interest, which is the case for other aromatics of the same size [25]. Under this assumption one can regard the excitation spectrum as being roughly proportional to an absorption spectrum of isolated fluoranthene.

An $S_1 \rightarrow S_0$ fluorescence excitation spectrum in the $S_0 \rightarrow S_1$ absorption region was also measured under exactly the same experimental conditions as the $S_0 \rightarrow S_4$ excitation spectrum. Since *no* hot bands but only a single narrow $S_{0,0} \rightarrow S_{1,0}$ transition at 25218 cm^{-1} was observed [26] the $S_0 \rightarrow S_4$ excitation spectrum in Fig. 2 must be due to fluoranthene molecules in the ground state $S_{0,0}$.

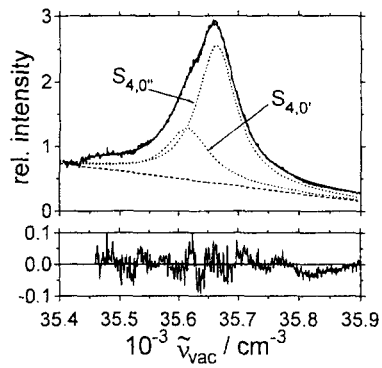

Fig. 3. Excitation spectrum of the $S_{1,v'} \rightarrow S_{0,v''}$ fluorescence of fluoranthene in a supersonic jet in the region of the 0, 0 transition of the $S_0 \rightarrow S_4$ absorption band. A linear background was assumed for the fit of two Lorentzian functions, represented by the dashed line (see parameters 1 and 2 in Table 1). The lower part shows the residuals of the total fit.

3.1. The origin of S_4

The strongest band at 35660 cm^{-1} (≈ 280 nm), shown in Fig. 3, is assigned to the symmetry-allowed $S_{0,0} \rightarrow S_{4,0}$ transition. The maximum of this band is blue-shifted by ≈ 360 cm^{-1} (≈ 2.6 nm) compared to fluoranthene in perfluoro-n-hexane at 293 K (see Fig. 1). A shift of this size is typical for measurements with inert solvents in comparison to gas phase experiments. [2] The range of the $S_{0,0} \rightarrow S_{4,0}$ absorption in jet-cooled fluoranthene is broad and not well defined. It consists of at least *two* transitions, $S_{0,0} \rightarrow S_{4,0'}$ at 35615 cm^{-1} and $S_{0,0} \rightarrow S_{4,0''}$ at 35664 cm^{-1}, which can be satisfactorily described by Lorentzian profiles with similar half-widths $\Gamma_{4,0'} \approx 89$ cm^{-1} and $\Gamma_{4,0''} \approx 79$ cm^{-1} as shown in Fig. 3 (see Table 1). The center of gravity of $S_{4,0'}$ and $S_{4,0''}$ is at 35644 cm^{-1}. The higher-energy part of the residuals in Fig. 3 indicates that perhaps a third function might improve the fit slightly.

3.1.1. The type of vibronic coupling $S_4 \Leftrightarrow S_3$

The energy gap between S_4 and S_3 of fluoranthene in solution (≈ 3750 cm^{-1}) is of an order of magnitude for which an intermediate-level structure is expected [19] (compare Section 1). The following observations support the classification of the $S_4 \Leftrightarrow S_3$ coupling as a *strong intermediate case*:

(1) The broad $S_{0,0} \rightarrow S_{4,0}$ band consists of at least two Lorentzian transitions.

(2) The part of the spectrum at the low-energy side of the $S_{4,0}$ band is structured. It consists of several transitions with an average separation of ≈ 50 cm^{-1} (upper limit for the mean separation ϵ_{eff}, cf. Section 1). These transitions carry roughly $\frac{1}{3}$ of the oscillator strength of the 0, 0 transition, which indicates an effective strong vibronic coupling $S_4 \Leftrightarrow S_3$.

(3) From the separation of the two 0, 0 transitions (≈ 49 cm^{-1}) and the ratio of their intensities a mean separation of the zeroth-order states ($\epsilon_{eff} \approx 20$ cm^{-1}) and the coupling matrix element ($V \approx 22$ cm^{-1}) can be estimated by first-order perturbation theory [28]. They meet criterion (1) for the strong intermediate case (cf. Section 1).

(4) The complex superposition of components of the intermediate-level structure [4–6], which replaces the 0, 0 transition typically spreads out over ≈ 100–300 cm^{-1} for other aromatic hydrocarbons [8,9]. The width of the $S_{4,0}$ band in Fig. 3, estimated with $\frac{1}{2}(\Gamma_{4,0'} + \Gamma_{4,0''}) + |\tilde{\nu}_{4,0''} - \tilde{\nu}_{4,0'}| \approx 133$ cm^{-1} is of that order of magnitude (see Table 1). The total

[2] In a Shpolskii matrix (n-hexane) at 5 K [27] the $S_{4,0}$ band is even shifted by ≈ 1000 cm^{-1} (≈ 9 nm) to lower wavenumbers compared to isolated fluoranthene.

Table 1
Spectroscopic data on the vibronic transitions $S_{0,0} \rightarrow S_{4,\nu}$ in fluoranthene

No.	Parameters of states $S_{4,\nu}$						
	$\tilde{\nu}_{4,\nu}$ (cm^{-1})	$\Delta\tilde{\nu}'_{4,\nu}$ (cm^{-1})	$\Delta\tilde{\nu}''_{4,\nu}$ (cm^{-1})	$I_{4,\nu}$	amplitude	$\Gamma_{4,\nu}$ (cm^{-1})	$\tau_{4,\nu}$ (fs)
1	35615	0		0.42	0.79	89	60
2	35664		0	1.00	2.12	79	67
3	35984	369	320	0.07	0.25	49	108
4	36094	479	430	0.01	0.05	50	106
5	36152	537	488	0.03	0.09	53	100
6	36197	582	533	0.15	0.38	64	83
7	36296	681	632	0.09	0.33	48	111
8	36438	823	774	0.04	0.17	42	126
9	36515	900	851	0.14	0.35	66	80
10	36633	1018	969	0.02	0.05	55	96
11	36691	1076	1027	0.05	0.19	47	113
12	36746	1131	1082	0.15	0.43	59	90
13	36828	1213	1164	0.07	0.17	66	80
14	36943	1328	1279	0.02	0.04	69	77
15	36968	1353	1304	0.29	0.68	71	75
16	37013	1398	1349	0.23	0.68	56	95
17	37071	1456	1407	0.37	0.92	67	79
18	37168	1553	1504	0.52	0.90	97	55
19	37287	1672	1623	0.20	0.37	89	60

Measured quantities: $\tilde{\nu}_{4,\nu}$: center wavenumbers of the fitted Lorentzian profile; $\Delta\tilde{\nu}'_{4,\nu}$: differences between $\tilde{\nu}_{4,\nu}$ and $\tilde{\nu}_{4,0'}$; $\Delta\tilde{\nu}''_{4,\nu}$: differences between $\tilde{\nu}_{4,\nu}$ and $\tilde{\nu}_{4,0''}$. The intensities $I_{4,\nu}$ are proportional to the areas of the vibronic lines and normalized to $I_{4,0''}$ (line 2). The amplitudes are the maxima of the Lorentzian profiles with respect to the corresponding local background. $\Gamma_{4,\nu}$: Lorentzian widths (fwhm) of transitions; $\tau_{4,\nu}$: lower limit for the lifetimes of vibronic states.

spread of the region of the origin including the structured part below the $S_{4,0}$ band is $\approx 600\ cm^{-1}$ (see Fig. 2).

(5) The background in the $S_0 \rightarrow S_4$ fluorescence excitation spectrum of fluoranthene is considerable and nearly constant over the entire spectral range. The major contribution to the background is due to an $S_{0,0} \rightarrow S_{3,w}$ absorption, based on the strong intermediate coupling. The contribution of the vibronic states $\{S_{1,v}\}$ and $\{S_{2,u}\}$ to the vibronic coupling is negligible, because of the large energy gap $\Delta E_{3,2}/hc \gtrsim 7000\ cm^{-1}$ in fluoranthene [20], which implies extremely small Franck–Condon vibrational overlap integrals between the molecular ground state $S_{0,0}$ and the highly vibrationally excited vibronic states $S_{2,u}$.

The vibrational structure of the excitation spectrum is strongly affected by the strong intermediate coupling of S_4 with S_3, as will be demonstrated in the following section.

3.2. The vibrational structure of S_4

To date only a few studies on the structure of the electronic states of fluoranthene exist in the literature [17–19,29]. The only study of jet-cooled fluoranthene is on S_1 [17], the vibrational structure of the ground state is treated in Ref. [18]. Fluoranthene possesses 72 fundamental modes, which are composed of 25 a_1 and 24 b_2 in-plane vibrations and of 11 a_2 and 12 b_1 out-of-plane vibrations, according to its C_{2v} symmetry [18]. The S_4 origin and fundamental modes of fluoranthene in S_4 are expected to be totally symmetric (a_1), since the electronic in-plane transition $S_0(A_1) \rightarrow S_4(A_1)$ is almost entirely polarized along the long two-fold z-axis of the molecule according to Kolc et al. [19]. [3] However, the linear

[3] The directions of the corresponding molecular axes, which were also chosen for fluoranthene by other authors [17–20,29], are shown in Fig. 1.

dichroic absorption spectrum of fluoranthene in polyethylene shows a weak band at the low-energy side of the $S_0 \rightarrow S_4$ transition, which is weakly polarized along the short y-axis. The $S_0 \rightarrow S_3$ transition is also mainly y-polarized. For these reasons and owing to the strong intermediate coupling non-totally symmetric in-plane modes (b_2) could also be observed in S_4. For an analysis of the vibrational structure of the excitation spectrum, Lorentzian profiles were fitted to all the distinct lines observed, in order to determine the central wavenumbers $\tilde{\nu}_{4,v}$ and linewidths $\Gamma_{4,v}$ of the vibronic states $S_{4,v}$. Lifetimes were evaluated using Eq. (4). To demonstrate the validity of the Lorentzian description of the lines, six profiles between 36000 and 36600 cm^{-1} are shown in Fig. 4. Energies and assignments of vibrational states in S_4 are compared with calculations and experimental results for the ground state S_0 (Raman and infrared spectra by Klaeboe et al. [18]), and with the vibrational energies in S_1 [17]. A compilation of all relevant parameters is listed in Table 1, assignments of the vibronic states $S_{4,v}$ and literature data are given in Table 2. All wavenumbers are vacuum corrected.

Due to the strong intermediate coupling of S_4 with S_3 the analysis of the vibrational structure of S_4 must be based on *both* components of the origin. The component $S_{4,0''}$ (line 2) is ≈ 2.6 times stronger than $S_{4,0'}$ (line 1) and is the most intense band of the entire spectrum. Consequently, the eigenstate $S_{4,0'}$ is less important for the vibrational structure of S_4. Wavenumbers of modes denoted with $'$ and $''$ (see Table 2) correspond to the two origins $S_{4,0'}$ and $S_{4,0''}$ respectively. One of the main features of the spectrum is the observation that lines 4, 5, 6, and lines 10, 11, 12 and 15, 16, 17 (respective wavenumbers are underlined in Table 2) are apparently mutually based on both origins. For the fundamental modes connected with these lines $v_i = v_i' \approx v_i''$ ($i =$ 3, 4, 9, 10, 12, 13) seems to hold; they occur in pairs (v_3, v_4), (v_9, v_{10}) and (v_{12}, v_{13}) in the spectrum. These pairs can be interpreted as repeating vibrational patterns of the two eigenstates forming the 0, 0 transition, similar to the repeating patterns of lines in the vibronic structure of $S_0 \rightarrow S_2$ in naphthalene [8]. Since the intensity of the lines is strongly dependent on the type of coupling it is not surprising that only the normalized intensity ratio of one pair (v_9/v_{10}, see Table 1) matches the ratio of the origin ($S_{4,0'}/S_{4,0''}$) well. If the interpretation of the vibrational patterns is correct, then the wavenumbers of modes connected with lines 4″, 6′, and lines 10″, 12′ and 15″, 17′ either coincide accidentally with certain S_4 fundamentals and/or combination of modes, or they are not relevant for the interpretation of the vibronic structure of the spectrum.

The dominant mode in S_4 is the fundamental mode v_1'' (line 3″) with $\tilde{\nu}_{4,v_1''} \approx 320$ cm^{-1}. It forms a harmonic progression over the entire spectral region studied. Mode v_1'' also occurs in several other combinations in that region. Chan and Dantus [17] found a fundamental mode in the $S_0 \rightarrow S_1$ fluorescence excitation spectrum at a wavenumber of ≈ 322 cm^{-1}, close to our value. Mode v_2'' (430 cm^{-1}) occurs in only a few combinations in the spectrum. It appears to be an extremely weak no progression-forming fundamental. In the fluorescence excitation spectrum of the first excited singlet state [17], however, combinations containing a fundamental mode at ≈ 427 cm^{-1} carry more than half the vibronic intensity. This difference is probably due to a significant change in the equilibrium geometry along the respective normal coordinate (the $S_0 \rightarrow S_1$ transition is mainly polarized perpendicular to the C_2 symmetry axis [20]). Mode v_2'' in S_4 is assigned as a totally symmetric mode (a_1). The energies of the totally symmetric modes v_3 (line 4′, 5″) and v_6'' (line 8″) match quite

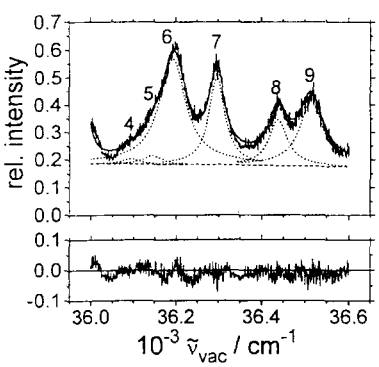

Fig. 4. Excitation spectrum of the $S_{1,v'} \rightarrow S_{0,v''}$ fluorescence of jet-cooled fluoranthene in the region of the vibronic transitions $S_{0,0} \rightarrow S_{4,v}$ for $v = 3$–8 (line 4 to 9). The solid line represents the sum of fitted Lorentzian profiles that are individually displayed with dotted lines. The residuals of the entire fit are shown in the lower part of the figure. A linear background represented by the dashed line was assumed for all fitted profiles.

Table 2
Assignments of fundamental modes, progressions and combinations relative to $S_{4,0'}$ (1′) and $S_{4,0''}$ (2″) at 35615 and 35664 cm^{-1} (compare Table 1)

No.	Assignments and comparison of $S_{4,i}$ modes								
	$\Delta\tilde{\nu}_{4,i}$ (cm^{-1})	[17] (cm^{-1}) exp.	[18] (cm^{-1}) calc.	[18] (cm^{-1}) Raman	[18] (cm^{-1}) IR	assignments fund.	assignments combinations	$\delta\tilde{\nu}$ (cm^{-1})	sym.
1′	0					$S_{4,0'}$			A_1 (?B_2)
2″	0					$S_{4,0''}$			A_1
3″	320	322	307	305	302	υ_1''			a_1
3′	(369)	365							
4″	430	427	413	429		υ_2''			a_1
4′	479	483	484	475	472	υ_3'			a_1
5″	488		484	475	472	υ_3''			a_1
5′	537	540				υ_4'			?b_2
6″	533	540				υ_4''			?b_2
6′	582	572	553		581	υ_5'			b_2
7″	632	654					$2\upsilon_1''$	+8	
7′	(681)								
8″	774	778	756	780	782	υ_6''			a_1
8′	823		806	804	801	υ_7'			a_1
9″	851	862					$2\upsilon_2''$	+9	
							$\upsilon_1'' + \upsilon_4$	+4	
9′	900		896	890		υ_8'	$\{\upsilon_1'' + \upsilon_5'\}$	+2	b_2
10″	969	968					$3\upsilon_1''$	−9	
							$\upsilon_2'' + \upsilon_4$	−4	
							$2\upsilon_3$	−2	
10′	1018	1028*	1018	1020		υ_9'	$\upsilon_3 + \upsilon_4$	+1	a_1
							$\{\upsilon_2'' + \upsilon_5'\}$	−6	
11″	1027	1028*	1018	1020		υ_9''	$\upsilon_3 + \upsilon_4$	−8	a_1
							$\{\upsilon_2'' + \upsilon_5'\}$	−15	
11′	1076	1074*	1104	1103	1104	υ_{10}'	$\upsilon_3 + \upsilon_5'$	−10	a_1
							$\{2\upsilon_1'' + \upsilon_2''\}$	−6	
12″	1082	1074*	1104	1103	1104	υ_{10}''	$\{\upsilon_3 + \upsilon_5'\}$	−16	a_1
12′	1131	1134*	1126	1136	1135	υ_{11}'	$\{2\upsilon_1'' + \upsilon_3\}$	−7	a_1
13″	1164	1153*					$\{2\upsilon_5'\}$	0	
							$2\upsilon_1'' + \upsilon_4$	+11	
13′	1213	1207					$\{2\upsilon_1'' + \upsilon_5'\}$	+9	
14″	1279						$4\upsilon_1''$	+1	
14′	1328						$\{\upsilon_1'' + \upsilon_2'' + \upsilon_5'\}$	+4	
15″	1304						$\{\upsilon_3 + \upsilon_7'\}$	+3	
							$\upsilon_4 + \upsilon_6''$	+5	
15′	1353	1351*	1318	1410	1410	υ_{12}'	$\{\upsilon_5' + \upsilon_6''\}$	+3	a_1
							$\{\upsilon_1'' + \upsilon_9\}$	−10	
							$\{\upsilon_1'' + \upsilon_3 + \upsilon_4\}$	−14	
16″	1349	1351*	1318	1410	1410	υ_{12}''	$\{\upsilon_5' + \upsilon_6''\}$	+7	a_1
							$\upsilon_1'' + \upsilon_9$	−6	
							$\upsilon_1'' + \upsilon_3 + \upsilon_4$	−10	
16′	1398	1400*	1431	1422	1420	υ_{13}'	$\upsilon_5' + \upsilon_7'$	+7	a_1
							$\{\upsilon_1'' + \upsilon_{10}\}$	+1	
							$\{2\upsilon_1'' + \upsilon_6''\}$	+16	
17″	1407	1400*	1431	1422	1420	υ_{13}''	$\{\upsilon_5' + \upsilon_7'\}$	−2	a_1
							$\upsilon_1'' + \upsilon_{10}$	−8	
							$2\upsilon_1'' + \upsilon_6''$	+7	
17′	1456	1481*	1467	1454	1452	υ_{14}'	$\{\upsilon_2'' + \upsilon_9\}$	−3	a_1

Table 2 (continued)

No.	Assignments and comparison of $S_{4,\,\iota}$ modes								
	$\Delta\tilde{\nu}_{4,\,\iota}$ (cm^{-1})	[17] (cm^{-1}) exp.	[18] (cm^{-1}) calc.	[18] (cm^{-1}) Raman	[18] (cm^{-1}) IR	assignments fund.	assignments combinations	$\delta\tilde{\nu}$ (cm^{-1})	sym.
18″	1504	1510*	1533	1529		υ''_{15}	$\upsilon''_2+\upsilon_{10}$	+5	a_1
							$\upsilon''_3+\upsilon_9$	+2	
							$3\upsilon''_1+\upsilon_4$	−9	
							$2\upsilon_3+\upsilon_4$	−2	
18′	1553	1588*	1580	1568		υ'_{16}	$2\upsilon_3+\upsilon'_5$	−4	b_2
							$\upsilon_3+\upsilon_{10}$	+10	
							$\{3\upsilon''_1+\upsilon'_5\}$	−11	
19″	1623	1600*	1636	1611		υ''_{17}	$\upsilon''_1+\upsilon_4+\upsilon''_6$	+6	a_1
19′	1672	1674*					$\{\upsilon''_1+\upsilon'_5+\upsilon''_6\}$	+4	
							$\upsilon'_5+\upsilon_{10}$	−11	
							$\upsilon'_5+\upsilon_{10}$	−11	

The numbers of the lines are marked with ′ and ″ respectively (column 1). Experimental values of wavenumbers $\Delta\tilde{\nu}_{4,\,\iota}$ (column 2) are compared with results from an $S_0 \rightarrow S_1$ fluorescence excitation spectrum by Chan and Dantus [17] (column 3), and with calculations and experimental data (Raman and infrared spectra) by Klaeboe et al. [18] (columns 4–6). Fundamental modes connected with the origins $S_{4,\,0'}$ and $S_{4,\,0''}$ are listed in column 7. Combinations of modes are shown in column 8. For combinations containing modes $\upsilon'_i \approx \upsilon''_i$ ($i = 3, 4, 9, 10$) wavenumbers $\tilde{\nu}_{4,\,\iota_i} = (\tilde{\nu}_{4,\,\iota'_i} + \tilde{\nu}_{4,\,\iota''_i})/2$ are taken. The differences $\delta\tilde{\nu}$ between experimental values $\Delta\tilde{\nu}_{4,\,\iota}$ and combinations of fundamental modes are listed in column 9; the assigned symmetries of the fundamental modes are shown in column 10. Wavenumbers in parentheses (column 2) represent modes for which reasonable assignments were not possible. Assignments in braces ({}, column 8) are mixed combinations. Wavenumbers maked with a '*' are combinations of fundamental modes in Ref. [17].

well the findings of Chan and Dantus [17], they also agree with the values given by Klaeboe et al. [18]. Modes υ_3 and υ''_6 occur in several combinations in the spectrum. Lines 4 and 5 are so weak (see Fig. 4 and Table 1) that the interpretation of υ_3 and υ_4 as a pair of fundamental modes is not necessarily justified, particularly because the rather strong adjacent line 6 appears difficult to interpret. On the one hand, line 6″ could be regarded as a fundamental υ''_4 which is connected to $S_{4,\,0''}$. It occurs in the spectrum as a progression-forming mode (cf. Table 2), which makes its interpretation as part of the pair (υ_3, υ_4) plausible. However, the calculated and experimental values by Klaeboe et al. [18] do not explain a totally symmetric mode at this particular wavenumber $\tilde{\nu}_{4,\,\upsilon''_4} \approx 533$ cm^{-1}. On the other hand, Klaeboe et al. observed a non-totally symmetric mode in the infrared spectrum at 581 cm^{-1}. Therefore, line 6′, which is based on the $S_{4,\,0'}$ origin (fundamental υ'_5, 582 cm^{-1}), can be interpreted as a non-totally symmetric b_2 mode, in agreement with the weakly y-polarized band in the linear dichroic spectrum by Kolc et al. [19] (see above). Combinations of υ'_5 occur throughout the spectrum particularly for lines that seem to be connected with the origin $S_{4,\,0'}$. The most obvious explanation for this observation and for the intensity of line 6′ would be the strong vibronic coupling of S_4 with S_3. As a consequence all combinations containing mode υ'_5 would gain part of their intensity from the strong vibronic $S_4 \Leftrightarrow S_3$ coupling. The weak fundamental υ_9 (line 10′, 11″) could alternatively be interpreted as a combination based on mode υ_4. The strong mode υ_{10} (line 11′, 12″) can be assigned to a totally symmetric fundamental, since assignment 12″ matches the findings in Ref. [18]. Within the range of the excitation spectrum no progressions or combinations based on modes υ_{13}, υ_{14}, υ''_{15} and υ''_{17} were observed so that an alternative interpretation of these fundamental modes as combinations may hold as well (cf. Table 2). Particularly, for mode υ''_{15} several combinations are conceivable. However, their high intensities corroborate their interpretation as fundamentals; especially mode υ_{13} was reported to be one of the strongest lines in the IR spectrum of fluoranthene [18]. Moreover, fundamental modes, typically corresponding to CC stretching modes of aromatic molecules, are expected to appear in this frequency

range (1300–1500 cm^{-1}). At excess energies $\gtrsim$ 1750 cm^{-1} the structure in the excitation spectrum becomes diffuse.

Most assignments are based on the comparison with ground state calculations and measurements; therefore, all conclusions drawn are only valid if the energies and symmetries of fundamental modes do not change considerably for different electronic states. This precondition is satisfied by the observation that the transition $S_{0,0} \rightarrow S_{4,0}$ is strong (indicating only slight changes in geometry in the electronically excited state). The total number of assigned fundamental modes forming the basis of the vibronic structure is probably too high. Several modes, which are tentatively assigned to fundamentals can be alternatively attributed to combinations of low-frequency modes. Several symmetry assignments are also purely tentative. Therefore, Table 2 should be regarded as a comprehensive collection of combinations and correlations within the vibronic structure of S_4.

3.2.1. Linewidths of vibronic states $S_{4,v}$

All half-widths of $S_{4,v}$ states are shown as a function of the corresponding center wavenumbers in Fig. 5 (see Table 1). Between 0 and 1500 cm^{-1} above the origin the linewidths pass through a minimum, which is observed at around 600 cm^{-1} above the origin. Broadening due to saturation effects (depletion of the ground state) was negligible because of low excitation fluences and the short lifetimes of the excited states $S_{4,v}$. The decrease in linewidths followed by a slow increase at higher excess energy

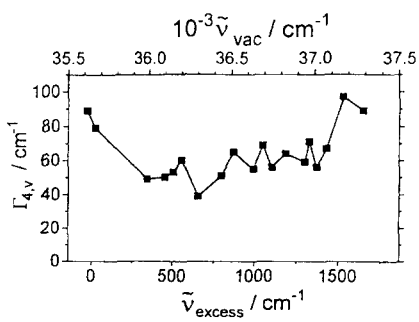

Fig. 5. Homogeneous half-widths (fwhm) $\Gamma_{4,v}$ of all assigned vibronic transitions $S_{0,0} \rightarrow S_{4,v}$ versus excess energy $\tilde{\nu}_{excess}$. The corresponding center wavenumbers $\tilde{\nu}_{4,v}$ are on the upper axis (see also Table 1).

can be understood by a gradual modification in the coupling mechanism from a strong intermediate case towards the statistical limit.

3.3. Calculation of the lifetime of S_4

Due to the strong intermediate coupling of S_4 with S_3, the lifetimes $\tau_{4,v}$ of lower vibronic states $S_{4,v}$ cannot be determined directly by the linewidth of the fitted Lorentzian profiles. The lifetimes $\tau_{4,v}$ given in Table 1, which are calculated with Eq. (4), represent only lower limits of the real lifetime (cf. Section 1). In a study of the delayed fluorescence from upper excited singlet states in solution [30] the lifetime of $S_{4,0}$ was estimated to be

$$\tau_{4,0} = \tau_{F4}^{*} \Phi_{S_1} \frac{DF_{S_4}}{DF_{S_1}} \approx 26 \text{ fs}, \qquad (5)$$

with $DF_{S_4}/DF_{S_1} \approx 4.2 \times 10^{-5}$ being the ratio of the delayed fluorescences (DF) from S_4 and S_1 [30]. The radiative lifetime $\tau_{F4}^{*} \approx 2.5$ ns was calculated from the integrated absorption spectrum in Ref. [30] and the $S_1 \rightarrow S_0$ fluorescence quantum yield $\Phi_{S_1} \approx 0.25$ was taken from Ref. [31]. Since inhomogeneous broadening due to solvent interactions is absent in a supersonic jet, τ_{F4}^{*} in Eq. (5) can be replaced by the true radiative lifetime τ_{F4} evaluated with Eq. (2). The number of components (m) replacing the zeroth-order 0, 0 transition is the crucial parameter in this estimate. The assumption of effectively two lines ($m = 2$) contributing to the 0, 0 band is supported by the good result of the two fitted Lorentzian profiles shown in Fig. 3 (lines 1 and 2 in Table 1), yielding a lifetime $\tau_{4,0} \approx 63$ fs according to Eq. (5), using a more recent value for $\Phi_{S_1} \approx 0.3$ [24]. The lifetimes $\tau_{4,0'} \approx 60$ fs (line 1, Table 1) and $\tau_{4,0''} \approx 67$ fs (line 2, Table 1) agree well with this calculation. This result ($m = 2$) is also supported by the similar value for the lifetime $\tau_{4,0} \gtrsim 50$ fs, which was evaluated in Ref. [30], [4] assuming rapid internal conversion to be the dominant relaxation pathway from S_4

[4] This lower limit of the lifetime of S_4 of fluoranthene ($\tau_{4,0} \gtrsim$ 50 fs) was calculated in conjunction with the objective of adequately treating the inhomogeneous broadening of spectra in solution due to fluctuations of the molecular environment.

in solution. In spite of the good agreement between lifetimes determined from linewidths in the excitation spectrum and lifetimes calculated with Eq. (5) and $\tau_{F4} \approx 5$ ns, the real number of effectively coupling states (m) may as well be slightly greater than 2. The residuals in Fig. 3 suggest that another Lorentzian component is likely to slightly improve the fit shown. This argument is supported by the structured $S_{3,w}$ background immediately below the 0, 0 transition, where a maximal energy spacing between effectively coupling states $\epsilon_{eff} \approx 50$ cm^{-1} was estimated from Fig. 2 (cf. Section 3.1). If this spacing is not drastically different in the adjacent region of the 0, 0 transition, the value for m will be $2 \lesssim m \lesssim 5$. The lifetime derived with Eq. (5) would be longer accordingly (63 fs $\lesssim \tau_{4,0} \lesssim$ 158 fs).

4. Conclusions

The excitation spectrum of the fluorescence from *highly* excited vibronic states $S_{1,v'} \rightarrow S_{0,v''}$ from jet-cooled fluoranthene was measured in the region of the $S_0 \rightarrow S_4$ absorption band. The following results were obtained.

(i) Up to excess wavenumbers of ≈ 1600 cm^{-1} above the S_4 origin at ≈ 35664 cm^{-1}, 19 vibronic transitions $S_{0,0} \rightarrow S_{4,v}$ were observed.

(ii) The $S_{0,0} \rightarrow S_{4,0}$ absorption band consists of at least two transitions, $S_{0,0} \rightarrow S_{4,0'}$ ($\Gamma_{4,0'} \approx 89$ cm^{-1}) and $S_{0,0} \rightarrow S_{4,0''}$ ($\Gamma_{4,0''} \approx 79$ cm^{-1}), whose contribution to the 0, 0 band can be described by purely Lorentzian line profiles.

(iii) The lower limits of the true radiative lifetime τ_{F4} and the lifetime $\tau_{4,0}$ of $S_{4,0}$ were estimated to be $\gtrsim 5$ ns and $\gtrsim 60$ fs, respectively.

(iv) In the overlapping region of the 0, 0 transition of the S_4 absorption band and the $\{S_{3,w}\}$ manifold, fluoranthene exhibits an intermediate-level structure. A strong intermediate vibronic coupling dominates the interaction between S_4 and S_3 over the whole spectral range studied.

(v) The most dominant mode in the vibrational structure is the totally symmetric low-energy mode v_1'' at ≈ 320 cm^{-1}. A non-totally symmetric mode v_5' at ≈ 581 cm^{-1} seems to play the central role as a promoting mode for the prevailing coupling mechanism.

Acknowledgement

We thank Professor J. Troe for supporting our work. We are grateful to Dr. B. Nickel for drawing our attention to the possibility of investigating the vibronic coupling of higher excited singlet states of aromatic hydrocarbons and for his experienced advice during this research project. We much appreciated valuable discussions on coupling mechanisms with Professor B. Dick (Universität Regensburg). We would like to thank Professor N. Ernsting (Humboldt Universität Berlin) for providing the jet apparatus, M. Gehring for the measurement of the absorption spectrum of fluoranthene and F. O'Keeffe and Dr. N. Heineking for critically reading the manuscript. Support by the Deutsche Forschungsgemeinschaft (Sonderforschungsbereich 357, Molekulare Mechanismen Unimolekularer Reaktionen) is gratefully acknowledged.

References

[1] A. Tramer and R. Voltz, in: Excited states, Vol. 4. ed. E.C. Lim (Academic Press, New York/London, 1979) p. 281.
[2] E.S. Medvedev and V.I. Osherov, Radiationless transitions in polyatomic moleclues (Springer-Verlag, Berlin/Heidelberg, 1995) ch. 2.5, 2.11.
[3] G.W. Robinson, in: Excited states, Vol. 1. ed. E.C. Lim (Academic Press, New York, 1974) p. 1.
[4] A.E. Douglas, J. Chem. Phys. 45 (1966) 1007.
[5] M. Bixon and J. Jortner, J. Chem. Phys. 50 (1969) 4061; M. Bixon and J. Jortner, J. Chem. Phys. 48 (1968) 715; M. Bixon and J. Jortner, J. Chem. Phys. 50 (1969) 3284.
[6] A. Nitzan, J. Jortner and P.M. Rentzepis, Proc. R. Soc. London Ser. A 327 (1972) 367.
[7] J. Wessel and D.S. McClure, Mol. Cryst. Liq. Cryst. 58 (1980) 121.
[8] S.M. Beck, D.E. Powers, J.B. Hopkins and R.E. Smalley, J. Chem. Phys. 73 (1980) 2019.
[9] A. Amirav, M. Sonnenschein and J. Jortner, J. Phys. Chem. 88 (1984) 5593.
[10] W.D. Lawrance and A.E.W. Knight, J. Phys. Chem. 94 (1990) 1249, and references therein.
[11] B. Dick and B. Nickel, Chem. Phys. 110 (1986) 131.
[12] G. Fischer, Chem. Phys. 4 (1974) 62.
[13] C.-J. Ho, R.J. Babbitt and MR. Topp, J. Phys. Chem. 91 (1987) 5599.
[14] R.J. Babbitt, C.-J. Ho and MR. Topp, J. Phys. Chem. 92 (1988) 2422.
[15] B. Nickel and M. Wick, Chem. Phys. 168 (1992) 111.
[16] M.T. Wick, B. Nickel and A.A. Ruth, Chem. Phys. Lett. 215 (1993) 243.

[17] I.Y. Chan and M. Dantus, J. Chem. Phys. 82 (1985) 4771.
[18] P. Klaeboe, S.J. Cyvin, A.P. Asbjornsen and B.N. Cyvin, Spectrochim. Acta A 37 (1981) 655.
[19] J. Kolc, E.W. Thulstrup and J. Michl, J. Am. Chem. Soc. 96 (1974) 7188.
[20] J. Michl, J. Mol. Spectrosc. 30 (1969) 66.
[21] N.P. Ernsting, J. Phys. Chem. 89 (1985) 4932.
[22] H. Hoyer and W. Peperle, Ber. Bunsenges. Phys. Chem. 62 (1958) 61.
[23] W.H. Melhuish, J. Opt. Soc. Am. 52 (1962) 1256.
[24] I.B. Berlman, H.O. Wirth and O.J. Steingraber, J. Am. Chem. Soc. 90 (1968) 566.
[25] A. Nakajima, Bull. Chem. Soc. Jpn. 45 (1972) 1687.
[26] M.T. Wick, Dissertation, University of Göttingen (1994).
[27] I.A. Nakhimovsky, M. Lamotte and J. Joussot-Dubien, Handbook of low temperature electronic spectra of polycyclic aromatic hydrocarbons (Elsevier, Amsterdam, 1989) p. 335.
[28] G. Herzberg, Molecular spectra and molecular structure, Vol. 2. Infrared and Raman spectra of polyatomic molecules (Van Nostrand Reinhold, New York, 1966) pp. 216, 266.
[29] L. Pesteil, P. Pesteil and F. Laurent, Can. J. Chem. 42 (1964) 2601.
[30] B. Nickel, Helv. Chim. Acta 61 (1978) 198.
[31] J.B. Birks, Photophysics of aromatic molecules (Wiley-Interscience, London, 1970) Table 4.3.